Bifunctionality of the thiamin diphosphate cofactor: assignment of tautomeric/ionization states of the 4′-aminopyrimidine ring when various intermediates occupy the active sites during the catalysis of yeast pyruvate decarboxylase

Anand Balakrishnan[||], **Yuhong Gao**[||], **Prerna Moorjani**[||], **Natalia S. Nemeria**[||], **Kai Tittmann**[⊥], and **Frank Jordan**[||]

[⊥]Albrecht-von-Haller Institute & Göttingen Center for Molecular Biosciences, Georg-August University Göttingen, D-37077 Göttingen, Germany

[||]Department of Chemistry, Rutgers University, Newark, NJ 07102, USA

Abstract

Thiamin diphosphate (ThDP) dependent enzymes perform crucial C-C bond forming and breaking reactions in sugar and amino acid metabolism and in biosynthetic pathways via a sequence of ThDP-bound covalent intermediates. A member of this superfamily, yeast pyruvate decarboxylase (YPDC) carries out the non-oxidative decarboxylation of pyruvate and is mechanistically a simpler ThDP enzyme. YPDC variants created by substitution at the active center (D28A, E51X, E477Q) and on the substrate activation pathway (E91D and C221E) display varying activity, suggesting that they stabilize different covalent intermediates. To test the role of both rings of ThDP in YPDC catalysis (the 4′-aminopyrimidine as acid-base, and thiazolium as electrophilic covalent catalyst), we applied a combination of steady state and time-resolved circular dichroism experiments (assessing the state of ionization and tautomerization of enzyme-bound ThDP-related intermediates), and chemical quench of enzymatic reaction mixtures followed by NMR characterization of the ThDP-bound intermediates released from YPDC (assessing occupancy of active centers by these intermediates and rate-limiting steps). Results suggest that: (1) Pyruvate and analogs induce active site asymmetry in YPDC and variants. (2) The rare 1′,4′-iminopyrimidine ThDP tautomer participates in formation of ThDP-bound intermediates. (3) Propionylphosphinate also binds at the regulatory site and its binding is reflected by catalytic events at the active site 20Å away. (4) YPDC stabilizes an electrostatic model for the 4′-aminopyrimidinium ionization state, an important contribution of the protein to catalysis. The combination of tools used provides time-resolved details about individual events during ThDP catalysis; the methods are transferable to other ThDP superfamily members.

INTRODUCTION

Yeast pyruvate decarboxylase (YPDC, EC 4.1.1.1), a thiamin diphosphate (ThDP) and Mg^{2+} dependent enzyme catalyzes the non-oxidative decarboxylation of pyruvate to acetaldehyde.

YPDC is an α_4 homotetramer of M_r 250,000 and is subject to activation by substrate [1] and by the substrate activator surrogate pyruvamide [2]. The cofactor ThDP is bound at the interface created by two monomers that form a tight dimer. This tight dimer known as the functional dimer is the minimal catalytically active unit [3–5] and two of these functional dimers assemble into a loose tetramer in the quaternary structure. X-ray crystallographic studies showed the coenzyme ThDP bound in the "V" conformation in the active sites of YPDC [6,7]. This unusual conformation of the ThDP brings the C2 and N4′ atoms within close contact (to less than 3.5 Å) of each other [8]. A consensus of chemical steps based on five decades of research on the YPDC catalyzed decarboxylation of pyruvate is shown in Scheme 1A, and involves a series of covalent ThDP-bound intermediates, including the pre-decarboxylation C2α-lactylThDP (LThDP), the enamine resulting from decarboxylation, and the post-decarboxylation C2α-hydroxyethylThDP (HEThDP) intermediates. The role of the 4′-aminopyrimidine ring in acid-base catalysis and activation of the thiazolium C2-H bond has been elucidated [9] aided by circular dichroism spectroscopic (CD) studies, providing evidence for the presence of not only the 4′-aminopyrimidine (AP form) but also of the 1′,4′-iminopyrimidine (IP) tautomeric form in YPDC catalysis. These CD studies suggested that in the LThDP and HEThDP intermediates with tetrahedral substitution at C2α the 1′,4′-iminopyrimidine IP tautomeric form predominates at pH values near and above the pK_a of the enzyme-bound 4′-aminopyrimidinium (APH$^+$) ionization state [10–15]. Concurrently, a complementary method using rapid acid quench of reaction mixtures in combination with ^{1}H NMR detection was developed; it is capable of quantification of the relative concentration of covalent ThDP-bound intermediates, and hence the relative rates of individual steps in the mechanism on many ThDP enzymes [16]. While both methods have some limitations (CD methods are limited by lack of direct absorption spectroscopic signatures for pyruvate-derived ThDP-bound covalent intermediates, the chemical quench NMR method does not provide information about the enzyme bound tautomeric form of the 4′-aminopyrimidine ring and cannot differentiate between the enamine and the HEThDP intermediate), a combination of the two methods could provide information about the state of ionization/tautomerization of the 4′-aminopyrimidine ring, and about the covalent ThDP-bound intermediates. This powerful combination enables us to gain insight to the catalytic contributions of both the 4′-aminopyrimidine and the thiazolium rings on ThDP enzymes as shown in Scheme 1A.

Two recent studies on ThDP enzymes also suggested that our understanding of the detailed role of the cofactor, of the conserved glutamate at the active centers, and of acid-base catalysis of ThDP enzymes is still incomplete. (1) The enzyme benzaldehyde lyase (BAL; EC 4.1.2.38) carries out reversible decomposition of (R)-benzoin to two molecules of benzaldehyde; in the reverse direction the enzyme is a carboligase. The BAL structure contained only two acid-base residues surrounding the ThDP at the active center [17–19]: the highly conserved E50 within hydrogen bonding distance of the N1′ atom of the 4′-aminopyrimidine ring, and the H29 residue. The residue H29 is too far from the thiazolium C2 atom to be useful in the first steps of the reaction, and was suggested to have a function in removing the β-hydroxyl proton of the ThDP-bound benzoin to assist release of the first benzaldehyde molecule. Because of the paucity of potential acid-base residues, the pH dependence of the steady-state kinetic parameters on BAL could be interpreted rather unambiguously: a residue was implicated in either the k_{cat}-pH or k_{cat}/K_M-pH profile with pK_a=5.3 at the acidic side, likely corresponding to the highly conserved glutamate residue [20] and providing the first pK_a value for this conserved glutamate. (2) The structure of the enzyme glyoxylate carboligase [(GCL; EC 4.1.1.47) carries out a carboligation reaction after decarboxylation of the first molecule of glyoxylate to the enamine intermediate] revealed even greater surprises. This enzyme is not only devoid of acid-base groups at its active center within hydrogen bonding distance of ThDP, *it is also lacking the highly conserved Glu*, in its place there is a hydrophobic valine residue [21].

To further our understanding of the various roles of the highly conserved glutamate and of other acidic amino acid residues implicated in the mechanism, we undertook steady state and transient state studies on YPDC variants produced earlier by substitutions at the catalytically important glutamate and aspartate residues (Figure 1), which are proposed to be involved in essential proton transfer steps [22,23]. Specifically, variants of: (i) the highly conserved E51 [believed to catalyze the tautomerization at the N1′ position of the cofactor [24]]; (ii) D28 and E477 [residues which assist in the protonation of the enamine and acetaldehyde release [3,22,25]] and (iii) C221 and E91 [the former is the locus of allosteric regulation [26,27], and the latter is situated at the interface of three domains and plays a central role in inter-domain communication from the allosteric β domain and C221 to the α domain (H92 the recipient of the information from pyruvate bound at C221) and thence the γ domain and the residues in a loop (residues 410–415) directly involved in ThDP binding [28–31]] were studied. To date, much of the information available on these YPDC variants is from steady state Michaelis-Menten kinetics and chemical quench NMR studies. Recently, phosphinate analogs of pyruvate have been shown to be excellent steric and electrostatic mimics of pyruvate and the most potent inhibitors of the pyruvate dependent E1 component of pyruvate dehydrogenase complexes [32]. In conjunction with CD experiments, detailed insights into the tautomeric states of intermediate analogs bound to YPDC under steady-state conditions and the rates of formation of such intermediates under pre-steady state conditions were obtained [10,33,34].

In this report, we use multiple strategies to gain further insight to catalysis by YPDC by interrogating key active center acid-base groups: CD to monitor accumulation of a stable LThDP intermediate analog and pyruvate-derived intermediates, and rapid quench NMR to assess rate-limiting steps with these variants. The combination of these strategies allowed direct detection of the covalent intermediates (via NMR) and the tautomeric state of the accompanying 4′-aminopyrimidine ring (via CD). Since the current methods allow us to study the events in the active sites containing ThDP, effect of these substitutions on individual catalytic steps could be determined and the role of these residues in YPDC catalysis could be assessed with greater certainty.

EXPERIMENTAL PROCEDURES

Materials

Alcohol dehydrogenase from yeast (ADH), β-mercaptoethanol (BME), β-NADH, Na_2EDTA, potassium phosphate, sodium pyruvate, morpholinoethanesulfonic acid (MES), phenylmethanesulfonyl fluoride (PMSF), thiamin hydrochloride and thiamin diphosphate were obtained from Sigma Chemical Company (St. Louis, MO). Dithiothreitol (DTT) and isopropyl-β-D-1-thiogalactopyranoside (IPTG) were from USB (Cleveland, OH).

Preparation of YPDC variants is described under Supporting Information.

Synthesis of sodium propionylphosphinate (PP) was recently published [35].

Enzyme purification

All variants were overexpressed in *E. coli* BL21(DE3) strain. YPDC, E91D, E51D, E51N, E51A and E477Q variants have a C-terminal His_6-tag and were purified using a Ni^{2+} Sepharose column [22,24]. The E51Q, D28A, D28N and, C221E variants that have no His_6-tag were purified as described elsewhere [22,36]. Protein concentration was determined by the Bradford method [37].

YPDC assays

Conversion of acetaldehyde to ethanol by yeast alcohol dehydrogenase in the presence of NADH was coupled to YPDC catalyzed production of acetaldehyde from sodium pyruvate. The disappearance of NADH is monitored at 340 nm using a Varian DMS 300 spectrophotometer [38]. The activity was measured in the presence of 20 mM pyruvate in standard assay buffer (50 mM MES, 1 mM ThDP, 2 mM MgCl$_2$, 0.2 mg/mL NADH, 0.08 mg/mL ADH, pH 6.0) at 30 °C. The reaction was started with addition of 3 μg/mL YPDC. For the variants, higher concentrations of enzyme were used.

Fluorescence spectroscopy to determine binding of ThDP and N1′-methylThDP to YPDC and E51A YPDC

The apo-E51A (3.0 mL, final concentration = 0.1 mg/mL) was first incubated with 0.003 mL Mg^{2+} (final concentration of 1 mM) and 2.697 mL of 100 mM MES, pH 6.0. Then aliquots of ThDP or N1′-methylThDP (NMThDP) were added and emission spectra were recorded from 300–450 nm. The experimental data were computer-fitted to the following equation [39],

$$(\Delta F/F_0 \times 100) = \frac{(\Delta F_{max}/F_0 \times 100) \cdot [S]}{K_d + [S]} \tag{1}$$

where $(\Delta F/F_0 \times 100)$ is the percent quenching (percent change in fluorescence relative to the initial value) following addition of ThDP or NMThDP at a concentration [S], and K_d is the dissociation constant. Fitting was carried out using nonlinear regression with the Marquardt-Levenberg algorithm (SigmaPlot, Jandel Scientific), providing values of K_d and $(\Delta F/F_0 \times 100)$.

Circular dichroism spectroscopy

All CD spectra were recorded on a Chirascan CD Spectrometer from Applied Photophysics (U.K.) in a 1 cm path length cell in the near–UV (280–400) wavelength region.

Titration experiments with propionylphosphinate (PP)

To 2.4 mL of YPDC or its variants in 20 mM MES (pH 6.0) containing 0.5 mM ThDP and 2.5 mM MgCl$_2$, an aliquot of PP from a 1M stock solution was added to achieve the desired concentration. The mixture was allowed to equilibrate for 1 min and the CD spectrum was recorded at 25 °C. The titration was performed over a PP concentration range of 0.5–40 mM. For quantitative analysis, the CD signal intensity of the IP (positive near 300 nm) and Michaelis complex (negative near 330 nm) bands corrected for dilution was plotted against PP concentration. Apparent dissociation constants (K_d^{app}) were calculated by fitting the data to a Hill function described in equation 2 using Sigmaplot v.7.0.

$$CD_{297} = CD_0 + \frac{CD_{297}^{max} \cdot [PP]^{n_H}}{(K_d^{app})^{n_H} + [PP]^{n_H}} \tag{2}$$

In this expression CD_{297} is the observed CD signal at the given wavelength, CD_0 the CD signal of the protein at this wavelength in the absence of PP, CD_{297}^{max} the maximum CD signal at saturation with PP, [PP] the concentration of substrate analog, and n_H the Hill coefficient.

Titration experiments with pyruvate

Experiments were performed with low activity variants and at 5 °C to slow down side reactions leading to carboligase products. To 2.4 mL of YPDC variants (2.75 mg/mL) at 5 °C in 20 mM MES (pH 6.0) containing 0.5 mM ThDP and 2.5 mM $MgCl_2$, an aliquot of pyruvate from a 1M stock solution was added to achieve the desired concentration. The mixture was stirred for 30 s and the CD spectrum was recorded at 5 °C. Additional aliquots of pyruvate were added until no further changes in CD spectra were observed.

Stopped-flow CD spectroscopy

Kinetic traces were recorded on a Pi*-180 stopped-flow CD spectrometer (Applied Photophysics, U.K.) using 10 mm path length at the specified wavelengths. Data were recorded at 302 nm for PP and at 313 nm for pyruvate experiments. Temperature was maintained at 10 °C for YPDC with pyruvate, and at 30 °C for YPDC variants with pyruvate experiments.

Pre-steady state formation of 1′,4′-iminopyrimidine tautomer of C2-(1-phosphino-1-propanol)ThDP

A solution of YPDC (8 mg/mL) in 20 mM MES (pH 6.0) containing 0.5 mM ThDP and 2.5 mM $MgCl_2$ in one syringe was mixed rapidly with an equal volume of PP (40 mM) in the same buffer placed in the second syringe. 20,000 data points were recorded over a period of 90 s. Data from six repetitive shots were averaged and the raw data were smoothed using the Savitsky-Golay function provided by the accompanying software and fit to a single-exponential model as in equation (3) using SigmaPlot v.7.0.

$$CD_{302}(t) = CD_1 \cdot e^{-k_1 t} + c \tag{3}$$

Pre-steady state formation of 1′4′-iminoLThDP and 1′4′-iminoHEThDP

A solution of YPDC (8 mg/mL) or variants in 20 mM MES (pH 6.0) containing 0.5 mM ThDP and 2.5 mM $MgCl_2$ in one syringe was mixed rapidly with an equal volume of pyruvate (40 mM) in the same buffer placed in the second syringe. 20,000 data points (2000 for YPDC) were recorded over a period of 2, 20 and 50 s for YPDC, E51D and E477Q variants, respectively. Data from ten repetitive shots were averaged and fit to a double-exponential model as in equation (4) using SigmaPlot v.7.0.

$$CD_{313}(t) = CD_1 \cdot e^{-k_1 t} + CD_2 \cdot e^{-k_2 t} + c \tag{4}$$

^{1}H NMR spectroscopy for detection of ThDP-bound intermediates

NMR spectra were acquired on a Varian 600 MHz instrument. The water signal was suppressed by pre-saturation. 4096 scans were collected with a recycle delay of 2.5 s, 32000 data points per scan, and 12 ppm spectral width.

Steady-state distribution of covalent ThDP intermediates in Glu51 variants

200 μL of E51 YPDC variants (E51D: 5 mg/mL; E51Q: 15 mg/mL; E51A: 24 mg/mL) in 20 mM MES (pH 6.0) was mixed with 200 μL of pyruvate (0.1 M) in the same buffer. In case of variant E51A, the buffer additionally contained 1 mM ThDP and 5 mM $MgCl_2$. The reaction was incubated at 25 °C for defined times assuring establishment of the true steady state (E51D and E51Q: 30 s, E51A: 180 s) and quenched with 200 μL of 12.5% TCA in 1M

DCl/D$_2$O. The mixture was centrifuged at 14,000 rpm for 30 min. and the supernatant was filtered through a Gelman Nylon Acrodisc (0.45 μm). The filtrate was used for ^{1}H NMR analysis as reported initially by Tittmann *et al.* [16] and on YPDC 291–300 loop variants by Joseph *et al* [40]. ThDP and ThDP-bound intermediates are stable under the acid quench conditions of the experiments (pH = 0.75). The ^{1}H chemical shift of the C6′-H resonances differ in various ThDP-bound intermediates and thus in a reaction mixture can be identified unambiguously, while their relative integrals provide a quantitative estimate of the relative abundance of the intermediates.

Transient state distribution of covalent ThDP intermediates in E51 variants

200 μL of E51 YPDC variants (E51D: 5 mg/mL; E51A: 24 mg/mL) in 20 mM MES (pH 6.0) was mixed with 200 μL of pyruvate (0.1 M) in the same buffer. In case of variant E51A, the buffer additionally contained 1 mM ThDP and 5 mM MgCl$_2$. Reaction was allowed to proceed for either 35 ms (E51D) or 2 s (E51A) and was then quenched with 200 μL of 12.5% TCA in 1M DCl/D$_2$O using a rapid quench instrument (RQF-3 from KinTek). Sample workup and NMR spectroscopic analysis was carried out as detailed in the previous paragraph[16,40].

Distribution of covalent ThDP intermediates in slow variants at 5 °C with low pyruvate concentration

400 μL of E477Q YPDC or E51D YPDC (25 mg/mL) in 20 mM MES (pH 6.0) containing 1 mM ThDP and 5 mM MgCl$_2$ was mixed with 50 μL of pyruvate (0.1 M). The reaction was incubated at 5 °C for 180 s and quenched with 200 μL of 12.5% TCA in 1M DCl/D$_2$O. Sample workup and NMR spectroscopic analysis was carried out as detailed in the previous paragraph[16,40].

RESULTS

Steady state kinetic studies of E51 YPDC variants

Due to the pronounced substrate-activation observed in the steady-state kinetics of YPDC, the data are discussed in terms of $S_{0.5}$, rather than K_M, as well as $k_{cat}/S_{0.5}$ (rather than k_{cat}/K_M) for the composite second order rate constant starting with addition of the first pyruvate to YPDC and culminating in the first irreversible step, decarboxylation of LThDP. The kinetic parameters for YPDC and the E51 variants (as well as for D28A, E477Q, C221E/C222A and E91D, other variants used in this study) are summarized in Table 1 (pH dependent kinetic data are presented in Figures S1 and S2 in Supporting Information). Substitutions at this position elicited decreases in k_{cat} from 1000-fold for E51D substitution to 10,000-fold for E51A and E51N substitutions as compared to the YPDC. Both the negative charge and the distance between the side chain of residue 51 and the N1′ atom of ThDP are important for catalytic activity. E51D, E51Q and E51N are still capable of forming a hydrogen bond with ThDP, albeit weaker, whereas H-bond formation is excluded in the E51A variant. The $S_{0.5}$ values also increase by an order of magnitude and a maximal value of 31 mM is observed for the E51N variant compared to 1.1 mM for YPDC, indicating that most substitutions at this position adversely affect substrate binding. The E51A variant displays anomalous behavior ($S_{0.5}$ = 0.72 mM), presumably reflecting the enlarged space. The one significant difference compared to an earlier report at this residue, is that in the current study, the E51A YPDC variant still retained non-zero residual activity [41].

Results from chemical quench followed by ^{1}H NMR detection of ThDP-bound covalent intermediates reveal that the events at the active sites follow a similar trend with YPDC and E51D, showing significant occupancy of the active sites with intermediates, whereas the E51Q variant shows much lower level of occupancy and intermediates do not accumulate at

detectable levels in the E51A variant (Figure 2). Clearly with the E51A variant, step(s) preceding addition of pyruvate to ThDP were rate limiting. Presumably, the activation of ThDP via formation of the APH[+] form is severely perturbed.

Binding of ThDP and NMThDP to E51A YPDC. Is there a binding preference for the charged APH[+] species?

To test the role of the E51 residue in cofactor binding, and possible stabilization of the APH[+] form on YPDC, a fluorescence titration experiment was carried out by reconstitution of apo-E51A YPDC with ThDP and NMThDP. On addition of ThDP or NMThDP to apo-E51A YPDC in 100 mM MES (pH 6.0) quenching of intrinsic fluorescence (excitation at 290 nm, emission at 338 nm) is observed. The quenching of apo-E51A YPDC fluorescence by ThDP was concentration-dependent and displayed saturation of half of the active centers only, with K_d of 27 µM (see Supporting info. Figure S3). In contrast, binding of NMThDP displayed saturation of all sites with K_d=5.4 µM. This experiment also suggests that the E51A substitution interrupts communication between active centers, resulting in saturation of only half of the sites by ThDP, such as was found with the corresponding E571A variant of *E. coli* pyruvate dehydrogenase E1[42]. Since the E51A has more space for the N1′-methyl group of the analog, the stronger binding of NMThDP than ThDP to this E51A variant is reasonable and clearly indicates that the 4′-aminopyrimidine ring contributes to binding. The experiments with NMThDP also imply that the 4′-aminopyrimidine-binding cleft is designed to stabilize the APH[+] form of ThDP electrostatically, as also found with the E571A variant of *E. coli* pyruvate dehydrogenase E1 [42]. This is the form, which can partition to the three neutral forms, AP, IP and the ylide in Scheme 1. Importantly, since no CD signatures are available for the APH[+] form, this experiment provides important support for the proposed notion.

Tautomeric forms of ThDP on YPDC observed with PP binding

Upon titration of YPDC with PP, two CD bands developed simultaneously: (i) a positive band at 297 nm and (ii) a negative band at 330 nm (Figure 3, top). The spectra were reminiscent of an analogous experiment with acetylphosphinate reported earlier [10]. The observed positive CD band at 297 nm could be assigned to the 1′,4′-iminopyrimidine tautomer (IP form) of C2-(1-phosphino-1-propanol)ThDP (PPThDP), and the negative CD band at 330 nm to a Michaelis complex consisting of enzyme, substrate analog and ThDP (Scheme 1B)[10–15]. Simultaneous development of both bands suggested that the four active sites exist in two distinct tautomeric/ionization states in the presence of PP, i.e., they are asymmetric. The titration data fit to the Hill equation revealed sigmoidal binding characteristics with Hill coefficients of 2.63 for the IP form of PPThDP and 2.13 for the Michaelis complex (Figure 3, bottom), suggesting that PP also binds at the regulatory sites and this binding event is recognized by the active sites. It is important to point out that the Michaelis complex is fully formed within the deadtime of the stopped flow instrument, while the rate of formation of the pre-decarboxylation intermediate or analog is on the stopped-flow time scale,

Allosteric activation is sensed by CD spectroscopy at the active sites

A CD titration of the E91D YPDC [the residue E91 is located on the α domain at the intersection of the three domains on the information transfer pathway emanating from the β domain (C221) to the γ domain (binding ThDP)], with PP, once more displayed simultaneous formation of two bands (Figure 4, top). However, the data fit to the Hill equation revealed hyperbolic binding characteristics with a Hill coefficient of 1.08 for the IP form of PPThDP and 1.5 for the Michaelis complex (Figure 4, middle). The K_d^{app} values, estimate of affinity of active sites for PP, were similar for this variant and YPDC (Table 2). The data indicate that the E91D YPDC retains its affinity for PP at the asymmetric active

sites notwithstanding disrupted communication with the regulatory site, as also seen earlier for pyruvate by Michaelis Menten kinetics [29].

In the C221E/C222A variant cysteine is replaced by glutamate, and this mimics pyruvate covalently bound to C221 in the hemithioacetal form, thus producing a permanently activated YPDC form. This variant showed only 2–5-fold reduction in activity compared to YPDC and hyperbolic Michaelis-Menten kinetics were observed [43]. In a CD titration experiment with PP, again both CD bands were observed but with reduced intensities (Figure 4, bottom). The titration data fit to the Hill equation revealed hyperbolic binding characteristics with a Hill coefficient of 1.0 for the IP form. Since with this substitution, PP cannot bind at the regulatory site of the enzyme, allosteric activation is completely abolished.

Active center substitutions severely impact PP binding

With the E51D substitution, addition of PP produces only the positive CD band at 297 nm (Figure 5, top) pertaining to the enzyme bound 1′,4′-iminoPPThDP intermediate, but gave no evidence of the negative CD band at 330 nm pertaining to the Michaelis complex. Titration data fit to the Hill equation revealed sigmoidal binding characteristics and a Hill coefficient of 2.74, similar to the value observed with YPDC. Allosteric regulation by PP is still seen in the formation of the tetrahederal intermediate analog. Apparently, the aspartate in E51D YPDC can still protonate the N1′ atom, a necessary step enroute to formation of the first tetrahederal (pre-decarboxylation) adduct and stabilization of the IP tautomer, however the stabilization of the Michaelis complex observed in the presence of substrate analog in YPDC is disrupted in this variant.

The residue D28 (α domain) and E477 (γ domain) are on different subunits and their substitutions disrupt the domain-domain (and subunit-subunit) interactions required for activity[7,8]. Upon titration of E477Q and D28A active-site variants with PP, only a weak positive CD band at 297 nm was observed in both cases (Figure 5 middle, bottom). but not the negative CD band at 330 nm. These active site substitutions severely affect: (i) PP binding (Michaelis complex formation) and (ii) formation of 1′,4′-iminoPPThDP with PP. Residues D28 and E477 are situated above the thiazolium ring in position to interact with the pyruvate carboxylate group. Their substitutions apparently affect the binding of PP in a productive conformation, which in turn also affect addition of thiazolium C2 to the carbonyl group of PP.

Tautomeric states of ThDP observed during catalytic cycle of YPDC variants with pyruvate

The low activity active center variants of YPDC (E51D, D28A, and E477Q) also accumulate intermediates under steady-state conditions and the rate of conversion between intermediates is slow. The tautomeric and ionization states of enzyme bound ThDP intermediates on the YPDC pathway could be determined using these variants. CD titration experiments were performed at 5 °C and pyruvate concentrations were in the range of 1–7 mM (typical $S_{0.5}$ range for these variants), to minimize production of chiral acetoin and/or acetolactate via the carboligase side reactions.

Addition of 1 mM pyruvate to the E477Q YPDC produced two CD bands: (i) broad positive band with CD_{max} at 297 nm for the IP form of a tetrahedral intermediate and (ii) broad negative band centered on 340 nm for the Michaelis complex (Figure 6, top). With further addition of pyruvate up to 5 mM, the bands showed negligible changes. The pyruvate induced active-site asymmetry observed in these spectra is similar to those observed on addition of PP in this work or acetylphosphinate to YPDC earlier[10]. This experiment confirms pyruvate-induced asymmetry of YPDC active sites.

Upon addition of 1 mM pyruvate to the E51D YPDC variant, similar to experiments with PP, a positive CD band with CD_{max} at 297 nm was evident for IP form of LThDP, while the negative CD band at ~330 nm was absent (Figure 6, middle). There was only a modest increase in amplitude upon further addition of 5 mM and even 20 mM pyruvate. Apparently, the pyruvate-induced Michaelis complex formation is severely disrupted in this variant suggesting that the residue Glu51 has a role in stabilizing the Michaelis complex. This observation also provides a physical explanation for the observed increase in $S_{0.5}$ for pyruvate for this variant (Table 1).

Neither CD band developed with significant amplitude on addition of 1 mM pyruvate to the D28A YPDC, and 7 mM pyruvate was needed to produce even weak bands - positive at 298 nm and negative at 328 nm (Figure 6, bottom). For this variant, the pyruvate-dependent acetaldehyde production plot exhibited remarkable characteristics: the rate of acetaldehyde production increases sharply and reaches a maximum at 2.5–3 mM pyruvate concentration, followed by a dramatic decrease, attributed to apparent substrate inhibition [25]. This variant produces acetolactate predominantly and C2-α-acetolactyl-ThDP (ALThDP) is the major intermediate under steady-state conditions, as determined by chemical quench/NMR previously [16]. To place these results into context, at low pyruvate concentrations, due to the low population of tetrahedral intermediates (alternatively, Michaelis complex and the enamine predominate), the CD band at 297 nm could not be observed. At high pyruvate concentrations ALThDP builds up (addition of enamine to a second molecule of pyruvate) reflected at 297 nm, the wavelength at which the ThDP-bound tetrahedral intermediates are seen in their IP form. While (S)-acetolactate, the predominant enantiomer produced by this variant shows a positive CD_{max} at 300 nm, no time dependence could be observed in the signal shown in the figure during course of the experiment at low pyruvate concentrations, affirming that no product was being formed during the experiment. Upon overnight incubation of the reaction mixture at 4 °C with 20 mM pyruvate, chiral (S)-acetolactate accumulated according to the positive CD_{max} at 300 nm.

Time-resolved spectroscopic studies on YPDC variants

Transient state kinetic studies of the formation of 1,4′-iminopyrimidine tautomer of ThDP-bound covalent intermediates—To determine kinetic competence of the covalent intermediate(s) in the IP tautomeric form observed earlier, rapid mixing experiments were performed. While the high turnover rate of YPDC precluded any steady-state CD experiments, pre-steady state experiments enabled detection of the IP tautomer at 313 nm upon mixing of YPDC with saturating concentrations of pyruvate (40 mM in syringe B). Time dependent accumulation of species with positive CD signal at 313 nm was observed and the process reached a steady state within 0.2 s with a rate constant of 312 s^{-1} (Figure 7, top). No time dependent changes could be observed for the Michaelis complex signal at 330 nm; presumably this intermediate accumulates within the 1.5 ms dead-time of the instrument, as observed earlier[44,50,,53]. Under substrate saturating conditions, when the rate of formation of Michaelis complex is very fast, the apparent rate of formation of LThDP intermediate approximates to the net forward rate constant k'_2 in Scheme 1A. This observed rate constant (312 s^{-1}) is in very good agreement with a previously determined k'_2 of 294 ± 20 s^{-1} for YPDC reaction with pyruvate [16]. This kinetic observation suggests that the IP tautomer being detected pertains to the LThDP tetrahedral intermediate. Further evidence obtained from NMR detection of intermediates at pre-steady state is presented below (Figure 8, bottom).

Transient state experiments performed with the E477Q and E51D active site variants (Figure 7, middle and bottom) revealed similar time dependent accumulation of species with positive CD signals at 313 nm, with the processes following biphasic kinetics with rate

constants of 0.4 and 0.04 s^{-1} for E477Q, and 1.2 and 0.08 s^{-1} for E51D. The rate constants are larger than the k_{cat} for these variants (Table 1) indicating that the intermediates detected are kinetically competent and transformation of these intermediates is probably among the rate limiting step(s). The biphasic kinetics observed most prominently in the case of E51D (both phases showing similar amplitudes of ~ 5 mdeg) also suggests the possibility of the variants showing differing kinetic competencies at differing time-scales.

The above observations of the kinetic fate of the IP tautomer were next tested by identification of the ThDP-bound covalent intermediates accompanying the IP tautomer by chemical quench coupled to NMR identification during both transient and steady state time-scales.

Chemical quench/NMR identification of ThDP-bound covalent intermediates
—^{1}H NMR spectra of samples of E51D YPDC and E477Q YPDC prepared under steady-state reaction conditions as described under experimental procedures revealed the presence of HEThDP and ThDP in the active sites (Figures 2,8,9). Relative integration of the C6′-H signals indicated that the active sites were filled with ~ 50% by HEThDP in both variants (Figures 2, and Figure 8 Top). HEThDP occupies most of the active sites during the steady state of YPDC with pyruvate [16]. Earlier reports showed that D28A YPDC in its reaction with pyruvate predominantly accumulates C2-α-acetolactylThDP, an intermediate also characterized on acetohydroxyacid synthase, and the E636Q variant of the *E. coli* pyruvate dehydrogenase E1 component [45,46]. These results allow straightforward assignments of CD observations as follows: (i) in E477Q YPDC, HEThDP in the IP form (~50%) and Michaelis complex (~50%); (ii) in E51D YPDC, HEThDP in the IP form (~50%); and (iii) in D28A YPDC, C2-α-acetolactylThDP in the IP form (~70%) and ~10–15% Michaelis complex.

A transient state sample prepared by quenching the YPDC - pyruvate reaction at 35 ms showed the presence of LThDP, HEThDP and ThDP (Figure 8, bottom two). The fraction of covalent intermediates is larger, indicating that under pre-steady state conditions most of the active sites contain covalent intermediates. Transient state samples prepared by quenching the E51D YPDC - pyruvate reaction showed the presence of LThDP, HEThDP and ThDP (Figure 9 top). The total occupancy of the covalent intermediates was ~50% (LThDP + HEThDP), indicating that under pre-steady state conditions half the active sites are occupied with varying covalent intermediates while the other half are possibly unoccupied (i.e., no Michaelis complex). In conjunction with the transient state kinetics, these results indicate that on YPDC the LThDP accumulates in its IP form at the measured rate constant of 311 s^{-1} during the transient state, while during the steady state the rate of decarboxylation of the accumulated LThDP becomes greater than its formation and thus only HEThDP/enamine accumulates. This analysis is extended also to transient state experiments on E51D YPDC, where both LThDP and HEThDP are detected by NMR analysis during pre-steady state (Figure 9) and HEThDP is detected during steady state (Figure 2). In this case LThDP accumulates in its IP form with a rate constant of 1.2 s^{-1}.

Interestingly, substitution of the conserved Glu51 residue does not affect accumulation of the IP tautomer in contrast to accumulation of the Michaelis complex (also note increased $S_{0.5}$ pyruvate and K_d^{app} for PP). The environment around N1′ still favors protonation but at a slower rate compared toYPDC. However, abolishing the acid residue as in E51A, produced a variant, which does not accumulate covalent intermediates at levels detectable by ^{1}H NMR (Figures 2 and 9). In this case, the N1′ protonation step is severely compromised thus slowing down ylide formation.

DISCUSSION

Homotropic allosteric regulation and co-operativity in YPDC

Compared to the other well-studied ThDP-dependent decarboxylase from *Zymomonas mobilis* (ZmPDC), the YPDC has an added complication arising from substrate activation[1,26–31,40,47]. The Rutgers group has participated in the determination of the X-ray structure of YPDC and in the elucidation of the substrate activation pathway. The cumulative evidence on the latter issue mapped the activation pathway to Cys221 on the β domain of the enzyme, to which the substrate could bind in a thiohemiacetal form, bridging to His92 then onto E91 (both on the α domain), thence to Trp412 of the ThDP binding loop on the γ domain (410 – 415) which also includes G413[28,29,31], the latter being hydrogen bonded to the 4′-amino group of ThDP, a group we have shown is involved in acid-base chemistry on the enzyme (Figure 1, bottom)[10–15].

While X ray structures provided direct evidence for large scale rearrangements in the quaternary and tertiary structures of activated YPDC and related non-oxidative decarboxylases [30,48,49], the current study probes the effect of these changes in the individual active-sites. Substitutions at C221 and E91 produced variants, which showed similar behavior to YPDC with PP (Michaelis complex, PPThDP and K_d^{app}) in CD experiments. However, with these substitutions, the binding curve was hyperbolic, indicating compromised communication between the allosteric and active sites (Table 2). These findings are similar to earlier results with Michaelis-Menten kinetics (Table 1), and in addition suggest that the allosteric regulation is achieved via control of individual steps starting with Michaelis complex formation.

While the substrate activation could be easily tested, the pathways involved in producing active site asymmetry are less clear. According to the 'proton-wire mechanism' for communication between active sites initially proposed by Frank et al. [50], and most recently experimentally supported on the E1 component of pyruvate dehydrogenase complex from *E. coli* [42], a direct pathway connecting the N1′ atoms of ThDP from two connected active-centers could be imagined for YPDC with the conserved Glu playing a prominent role. This would be different from the pathway suggested in ref. 50 since the direct pathway between two E51 residues in a functional dimer also includes residues capable of hydrogen bonding, but not of proton shuttling (Supporting Information Figure S5). Replacing glutamate by aspartate in E51D variant produced CD spectra reminiscent of other ThDP enzymes with non-communicating active sites, i.e., no Michaelis complex was observed. However, the increased $S_{0.5}$ for E51 variants and K_d^{app} of PP for E51D suggest that the substitutions produce variants with reduced ability to stabilize the Michaelis complex.

Michaelis complex in YPDC catalysis

The Michaelis complex, observed as a negative CD band at 330 nm in the presence of pyruvate or PP, is the non-covalent enzyme substrate/substrate analog intermediate in YPDC catalysis (Scheme 1A and 1B). The Michaelis complex is proposed to comprise the enzyme bound ThDP and a pyruvate molecule bound to the active-site as detected on variants of the E1p component of *E. coli* pyruvate dehydrogenase complex with low catalytic activity[44,50,53]. However, this intermediate does not accumulate upon titration of either parental E1p or pyruvate oxidase with PP (see Supporting Information Figure S4). The present study with YPDC variants provides some insight into the minimal conditions necessary for accumulation of the Michaelis complex at levels detectable by CD spectroscopy.

YPDC, its E91D and C221E variants stabilize the Michaelis complex in the presence of acetylphosphinate, methyl acetylphosphonate [10,14] and PP. However, substitutions at the

active site perturb the stabilization of this intermediate. The residue Glu51 appears to be necessary for stabilization of the enzyme-ThDP-pyruvate or enzyme-ThDP-PP Michaelis complex. Considering the conserved role of this residue in protonation of the N1′ position of the 4′-aminopyrimidine ring, it can be concluded that the APH$^+$ state of ThDP is an essential component of the Michaelis complex. The D28A and E477Q variants failed to accumulate the Michaelis complex upon titration with PP. These residues are positioned above the thiazolium ring closer to the pyruvate-binding site. Perturbations at these positions possibly affect optimal binding of PP in the active site and thus preclude formation of the Michaelis complex. Together, these observations suggest that ThDP in its APH$^+$ state (its activated state on enzymes[52]), and substrate bound at the active sites, in an orientation probably guided by the residues E477 and D28, are required for detection of the Michaelis complex by CD.

With pyruvate however, the E477Q and D28A variants do accumulate the Michaelis complex to varying extents indicating that pyruvate binds to the active site in the near attack conformation in these variants albeit with perturbations. Approximately 50% of the active sites in E477Q YPDC and 10–15% active sites in D28A YPDC are in the Michaelis complex form in a reaction with pyruvate according to NMR analysis of steady-state intermediate distribution. Possibly, the fact that PP is one CH_2 group longer than pyruvate, and the additional space needed on replacement of the trigonal carboxylate by the tetrahedral phosphorus environment, account for the difference in the behavior of PP compared to pyruvate.

1′,4′-Iminopyrimidine tautomer of ThDP in YPDC catalysis

The 1′,4′-iminopyrimidine tautomeric form of ThDP has been shown to accompany tetrahedral pre-decarboxylation intermediate analogs in 10 different members of the ThDP superfamily of enzymes to date. Also, the 1′,4′-iminopyrimidine tautomeric form of ThDP was previously shown to accumulate during HEThDP formation in the reversible reaction with acetaldehyde on YPDC[15]. The current study *for the first time* provides evidence for formation of such intermediate in the forward direction of catalysis with pyruvate. While the steady-state CD spectroscopy experiments pointed toward accumulation of 1′,4′-imino-HEThDP in the E51D and E477Q variants, chemical quench/NMR analysis at various time scales afforded snapshots of tetrahedral intermediate distribution during both steady-state and pre-steady state phases. Rate constants for LThDP formation on YPDC from NMR analysis, and rate constant for formation of 1′,4′-iminopyrimidylLThDP from transient state CD spectroscopy are in very good agreement within experimental error; during short time-scales the 1′,4′-iminopyrimidylLThDP was detected and kinetically characterized in the forward reaction.

Evidence for active-site asymmetry in the presence of pyruvate was found from experiments with E477Q YPDC and D28A YPDC during steady state. The co-existence of both pre-decarboxylation and post-decarboxylation intermediates in YPDC active sites is in agreement with a previous prediction by a model for alternating sites mechanism of catalysis of YPDC[54]. Additionally, detection of the IP form of ThDP in the presence of C2α-acetolactylThDP in D28A YPDC active sites provides further support for the notion that all tetrahedral C2α-substituted ThDP intermediates are in the IP form at pH values near and above the pK_a of the APH$^+$ form. Direct observation of the APH$^+$ form on three ThDP enzymes was recently achieved by solid state NMR methods[52].

CONCLUSION

To conclude, a summary of findings of this report is presented in Table 3, which clearly demonstrates the strength of combining steady state and transient state CD and ^{1}H NMR

methods to elucidate individual steps on the reaction pathway (Scheme 1). There is now the possibility to obtain an ever more detailed microscopic picture of the pathway and to assign function to key amino acid residues on other ThDP enzymes with greater certainty.

Supplementary Material

Refer to Web version on PubMed Central for supplementary material.

Acknowledgments

ABBREVIATIONS

ThDP	thiamin diphosphate
YPDC	wild type yeast pyruvate decarboxylase (EC 4.1.1.1) isolated from *Saccharomyces cerevisiae*
E51D, E51N, E51Q and E51A, D28A, D28N, E477Q, C221E, and E91D	variants at the indicated positions of YPDC
ZmPDC	pyruvate decarboxylase from *Zymomonas mobilis*
E1p	first enzymatic component of the *E. coli* pyruvate dehydrogenase complex
LThDP	C2α-lactylthiamin diphosphate
HEThDP	C2α-hydroxyethylthiamin diphosphate
PLThDP	C2α-phosphonolactylthiamin diphosphate
NMThDP	N1′-methylthiamin diphosphate
CD	circular dichroism
AP	4′-aminopyrimidine form of ThDP
IP	1′,4′-iminopyrimidine form of ThDP
APH⁺	N1′-protonated 4′-aminopyrimidinium form of ThDP
PP	propionylphosphinate sodium salt
PPThDP	C2-(1-phosphino-1-propanol)thiamin diphosphate the adduct of propionylphosphinate and ThDP
MES	morpholinoethanesulfonic acid

References

1. Boiteux A, Hess B. FEBS Lett. 1970; 9:293. [PubMed: 11947696]
2. Hubner G, Konig S, Schellenberger A. Biomed Biochim Acta. 1988; 47:9. [PubMed: 3291865]
3. Sergienko EA, Jordan F. Biochemistry. 2002; 41:6164. [PubMed: 11994012]
4. Konig S, Svergun D, Koch MH, Hubner G, Schellenberger A. Eur Biophys J. 1993; 22:185. [PubMed: 8404724]
5. Killenberg-Jabs M, Jabs A, Lilie H, Golbik R, Hubner G. Eur J Biochem. 2001; 268:1698. [PubMed: 11248689]

6. Muller YA, Lindqvist Y, Furey W, Schulz GE, Jordan F, Schneider G. Structure. 1993; 1:95. [PubMed: 8069629]

7. Dyda F, Furey W, Swaminathan S, Sax M, Farrenkopf B, Jordan F. Biochemistry. 1993; 32:6165. [PubMed: 8512926]

8. Arjunan P, Umland T, Dyda F, Swaminathan S, Furey W, Sax M, Farrenkopf B, Gao Y, Zhang D, Jordan F. J Mol Biol. 1996; 256:590. [PubMed: 8604141]

9. Schellenberger A. Biochim Biophys Acta. 1998; 1385:177. [PubMed: 9655906]

10. Nemeria N, Chakraborty S, Baykal A, Korotchkina LG, Patel MS, Jordan F. Proc Natl Acad Sci U S A. 2007; 104:78. [PubMed: 17182735]

11. Jordan F, Nemeria NS, Zhang S, Yan Y, Arjunan P, Furey W. Journal of the American Chemical Society. 2003; 125:12732. [PubMed: 14558820]

12. Baykal AT, Kakalis L, Jordan F. Biochemistry. 2006; 45:7522. [PubMed: 16768448]

13. Jordan F, Zhang Z, Sergienko E. Bioorg Chem. 2002; 30:188. [PubMed: 12406703]

14. Nemeria N, Baykal A, Joseph E, Zhang S, Yan Y, Furey W, Jordan F. Biochemistry. 2004; 43:6565. [PubMed: 15157089]

15. Nemeria NS, Chakraborty S, Balakrishnan A, Jordan F. FEBS J. 2009; 276:2432. [PubMed: 19476485]

16. Tittmann K, Golbik R, Uhlemann K, Khailova L, Schneider G, Patel M, Jordan F, Chipman DM, Duggleby RG, Hubner G. Biochemistry. 2003; 42:7885. [PubMed: 12834340]

17. Brandt GS, Nemeria N, Chakraborty S, McLeish MJ, Yep A, Kenyon GL, Petsko GA, Jordan F, Ringe D. Biochemistry. 2008; 47:7734. [PubMed: 18570438]

18. Maraite A, Schmidt T, Ansorge-Schumacher MB, Brzozowski AM, Grogan G. Acta Crystallogr Sect F Struct Biol Cryst Commun. 2007; 63:546.

19. Mosbacher TG, Mueller M, Schulz GE. FEBS J. 2005; 272:6067. [PubMed: 16302970]

20. Nemeria N, Korotchkina L, McLeish MJ, Kenyon GL, Patel MS, Jordan F. Biochemistry. 2007; 46:10739. [PubMed: 17715948]

21. Kaplun A, Binshtein E, Vyazmensky M, Steinmetz A, Barak Z, Chipman DM, Tittmann K, Shaanan B. Nat Chem Biol. 2008; 4:113. [PubMed: 18176558]

22. Liu M, Sergienko EA, Guo F, Wang J, Tittmann K, Hubner G, Furey W, Jordan F. Biochemistry. 2001; 40:7355. [PubMed: 11412090]

23. Sergienko EA, Jordan F. Biochemistry. 2001; 40:7382. [PubMed: 11412092]

24. Gao, Y. PhD Dissertation. Rutgers University; 2000.

25. Sergienko EA, Jordan F. Biochemistry. 2001; 40:7369. [PubMed: 11412091]

26. Baburina I, Dikdan G, Guo F, Tous GI, Root B, Jordan F. Biochemistry. 1998; 37:1245. [PubMed: 9477950]

27. Baburina I, Gao Y, Hu Z, Jordan F, Hohmann S, Furey W. Biochemistry. 1994; 33:5630. [PubMed: 8180188]

28. Li H, Jordan F. Biochemistry. 1999; 38:10004. [PubMed: 10433707]

29. Li H, Furey W, Jordan F. Biochemistry. 1999; 38:9992. [PubMed: 10433706]

30. Jordan F, Nemeria N, Guo F, Baburina I, Gao Y, Kahyaoglu A, Li H, Wang J, Yi J, Guest JR, Furey W. Biochim Biophys Acta. 1998; 1385:287. [PubMed: 9655921]

31. Baburina I, Li H, Bennion B, Furey W, Jordan F. Biochemistry. 1998; 37:1235. [PubMed: 9477949]

32. Nemeria NS, Korotchkina LG, Chakraborty S, Patel MS, Jordan F. Bioorg Chem. 2006; 34:362. [PubMed: 17070897]

33. Meyer D, Neumann P, Parthier C, Friedemann R, Nemeria N, Jordan F, Tittmann K. Biochemistry. 2010; 49:8197. [PubMed: 20715795]

34. Chakraborty, S. PhD Dissertation. Rutgers: the State University of New Jersey; 2006.

35. Shim DJ, Nemeria NS, Balakrishnan A, Patel H, Song J, Wang J, Jordan F, Farinas ET. Biochemistry. 2011

36. Wang J, Golbik R, Seliger B, Spinka M, Tittmann K, Hubner G, Jordan F. Biochemistry. 2001; 40:1755. [PubMed: 11327837]

37. Bradford MM. Anal Biochem. 1976; 72:248. [PubMed: 942051]

38. Holzer H, Schultz G, Villar-Palasi C, Juntgen-Sell J. Biochem Z. 1956; 327:331. [PubMed: 13328844]

39. Liu R, Sharom FJ. Biochemistry. 1996; 35:11865. [PubMed: 8794769]

40. Joseph E, Wei W, Tittmann K, Jordan F. Biochemistry. 2006; 45:13517. [PubMed: 17087505]

41. Killenberg-Jabs M, Konig S, Eberhardt I, Hohmann S, Hubner G. Biochemistry. 1997; 36:1900. [PubMed: 9048576]

42. Nemeria NS, Arjunan P, Chandrasekhar K, Mossad M, Tittmann K, Furey W, Jordan F. J Biol Chem. 2010; 285:11197. [PubMed: 20106967]

43. Wei W, Liu M, Jordan F. Biochemistry. 2002; 41:451. [PubMed: 11781083]

44. Kale S, Arjunan P, Furey W, Jordan F. J Biol Chem. 2007; 282:28106. [PubMed: 17635929]

45. Tittmann K, Schroder K, Golbik R, McCourt J, Kaplun A, Duggleby RG, Barak Z, Chipman DM, Hubner G. Biochemistry. 2004; 43:8652. [PubMed: 15236573]

46. Nemeria N, Tittmann K, Joseph E, Zhou L, Vazquez-Coll MB, Arjunan P, Hubner G, Furey W, Jordan F. J Biol Chem. 2005; 280:21473. [PubMed: 15802265]

47. Hubner G, Weidhase R, Schellenberger A. Eur J Biochem. 1978; 92:175. [PubMed: 365531]

48. Kutter S, Weiss MS, Wille G, Golbik R, Spinka M, Konig S. J Biol Chem. 2009; 284:12136. [PubMed: 19246454]

49. Versees W, Spaepen S, Wood MD, Leeper FJ, Vanderleyden J, Steyaert J. J Biol Chem. 2007; 282:35269. [PubMed: 17905741]

50. Frank RA, Titman CM, Pratap JV, Luisi BF, Perham RN. Science. 2004; 306:872. [PubMed: 15514159]

51. Jordan F, Arjunan P, Kale S, Nemeria NS, Furey W. J Mol Catal B Enzym. 2009; 61:14. [PubMed: 20160956]

52. Balakrishnan A, Paramasivam S, Chakraborty S, Polenova T, Jordan F. J Am Chem Soc. 2012; 134:665. [PubMed: 22092024]

53. Kale S, Ulas G, Song J, Brudvig GW, Furey W, Jordan F. Proc Natl Acad Sci USA. 2008; 105:1158. [PubMed: 18216265]

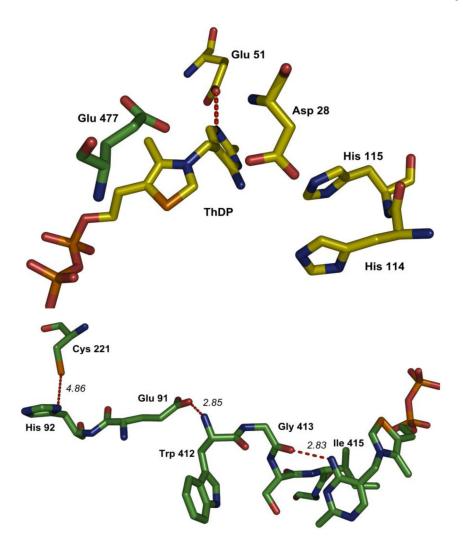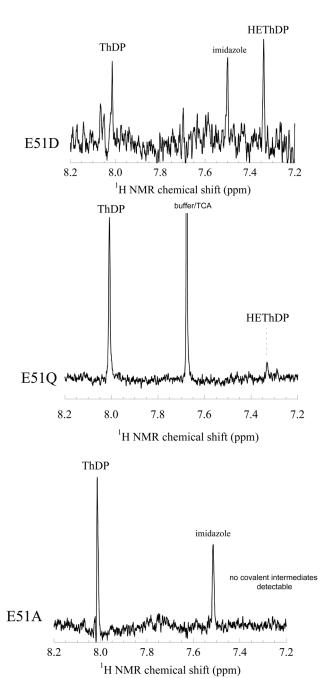54. Sergienko EA, Jordan F. Biochemistry. 2002; 41:3952. [PubMed: 11900538]

Figure 1.
ThDP bound in the V confirmation at the active site of YPDC. (Top) Side chains of residues which potentially participate in proton transfer steps (Glu51, Glu477, Asp28, His114, and His 115) are shown. (Bottom) Connectivity between Cys221 at the regulatory site and the ThDP binding loop (410–415) via His92, Glu91, and backbone N and O atoms of Trp412 and Gly413. Coordinates were taken from the PVD1.pdb file and illustrated using Pymol.

Figure 2.
Distribution of ThDP covalent intermediates of Glu51 variants during steady state. C6′-H fingerprint region in ^{1}H NMR spectra acquired with after acid quench of the reaction of (Top) E51D YPDC (5 mg/mL) (middle) E51Q (15 mg/mL) and (bottom) E51A (24 mg/mL) with 100 mM pyruvate. All spectra were acquired at 25 °C and pH 0.75. Acquisition parameters are described under Experimental Procedures.
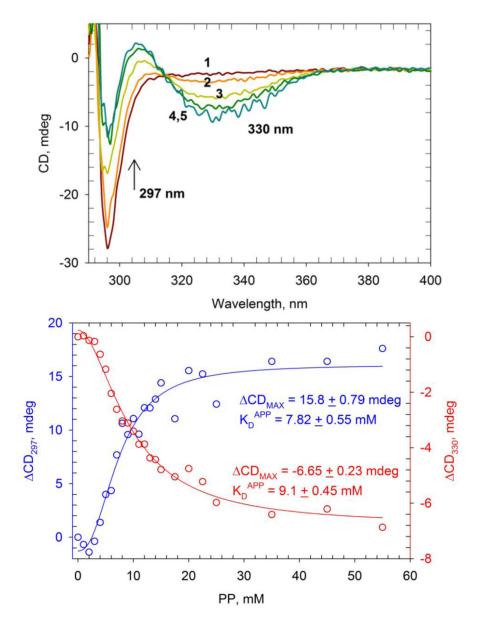
Figure 3.
Formation of 1′ 4′-iminoPPThDP on YPDC. (Top): Near UV (290 – 400 nm) CD spectra of YPDC (5.0 mg/mL) in absence of PP (1) and in presence of 5 mM PP (2), 10 mM PP (3), 20 mM PP (4) and 35 mM PP (5). The 1′,4′-iminoPPThDP species (Scheme 1B) is seen accumulating at 297 nm and the Michaelis complex (YPDC + PP) is seen accumulating at 330 nm. (Bottom): CD amplitude of IP form at 297 nm (blue circles) and of Michaelis complex at 330 nm (red circles) during titration plotted against concentration of PP.
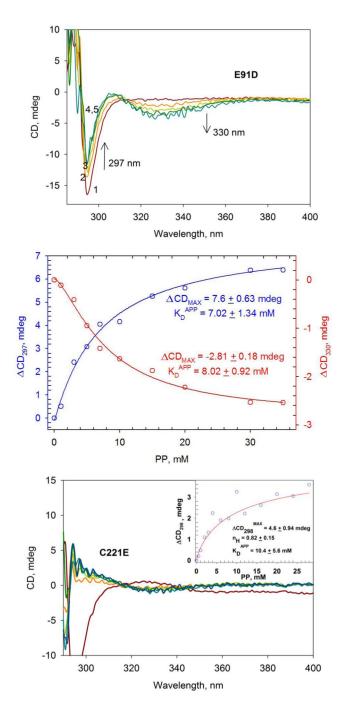
Figure 4.
Formation of 1′, 4′-iminoPPThDP on the E91D and C221E/C222A substrate activation pathway variants. (Top): Near UV (290 – 400 nm) CD spectra of titration of E91D YPDC (2.75 mg/mL) (1) and in presence of 5 mM PP (2), 10 mM PP (3), 20 mM PP (4) and 35 mM PP (5). The 1′, 4′-iminoPPThDP species is seen accumulating at 297 nm and the Michaelis complex at 330 nm. (Middle): CD amplitude of IP form at 297 nm (blue circles) and of Michaelis complex at 330 nm (red circles) plotted against concentration of PP. The data points were fitted to the Hill equation and the regression fit lines are displayed. (Bottom): Near UV (290 – 400 nm) CD spectra of C221E/C222A YPDC (2.75 mg/mL) (brown). Difference spectra obtained after subtraction of spectrum in the absence of PP from

those in presence of 1–28 mM of PP. The 1′,4′-iminoPPThDP species is seen accumulating at 298 nm. (Inset) Dependence of CD amplitude at 298 nm on PP concentration. The data points (circles) were fitted to a Hill equation and the regression fit line is displayed.
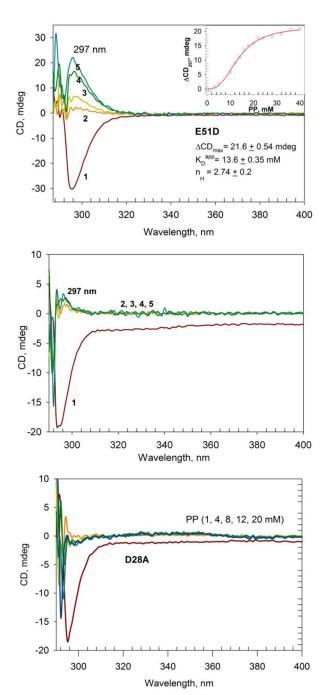
Figure 5.
Formation of 1′, 4′-iminoPPThDP on D28A, E51D and E477Q active site variants. (Top): Near UV (290 – 400 nm) CD spectrum of E51D YPDC (5.0 mg/mL) (1). Difference spectra obtained after subtraction of (1) from spectra in the presence of 5 mM (2) 10 mM (3) 20 mM (4) and 40 mM (5) PP. The 1′,4′-iminoPPThDP species is seen accumulating at 297 nm. (Inset) Dependence of signal amplitude at 297 nm on PP concentration. The data points (circles) were fitted to a Hill equation and the regression fit line is displayed. (Middle): Near UV (290 – 400 nm) CD spectrum of E477Q YPDC (2.75 mg/mL) (1). Difference spectra obtained after subtraction of (1) from those in the presence of: 5 mM (2) 10 mM (3), 20 mM (4) and 40 mM (5) PP. The 1′,4′-iminoPPThDP species is seen accumulating at 297 nm.

(Bottom): Near UV (290 – 400 nm) CD spectrum of D28A YPDC (2.75 mg/mL) (brown). Difference spectra obtained after in the presence 4–20 mM of PP.
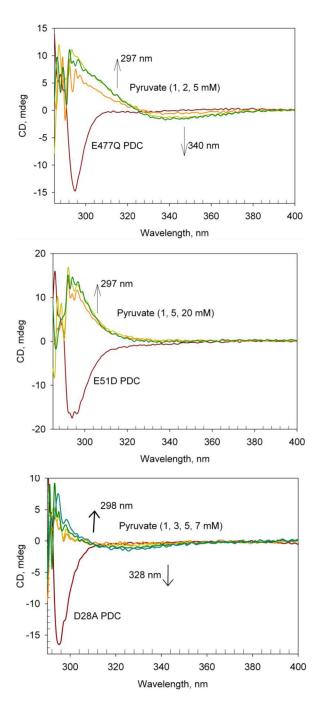
Figure 6.
Formation of 1′, 4′-iminoLThDP and Michaelis complex on the D28A, E51D and E477Q active site variants from pyruvate under steady state. Near UV (290 – 400 nm) CD spectra of (Top): E477Q YPDC (2.75 mg/mL) (brown) and difference spectra in the presence of pyruvate (1, 2 and 5 mM). (Middle): E51D YPDC (2.75 mg/mL) and difference spectra in the presence of pyruvate (1, 5 and 20 mM). (Bottom): D28A YPDC (2.75 mg/mL) (brown) and difference spectra in the presence of pyruvate (1, 3, 5 and 7 mM). In all cases the positive CD band with maxima at 297 nm pertains to the 1′,4′-imino tautomer of a tetrahedral ThDP-bound intermediate, LThDP. The negative CD band centered at ~ 330 nm pertains to the Michaelis complex and is absent in spectra of E51D YPDC.
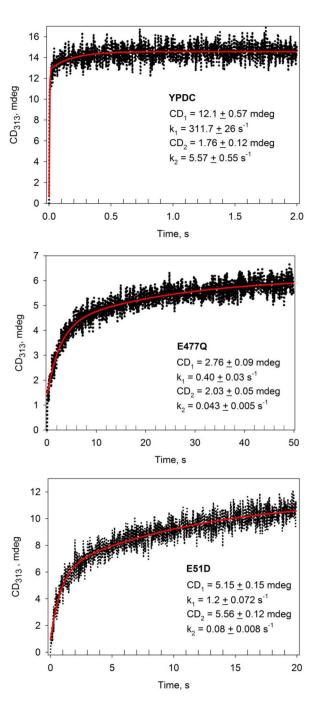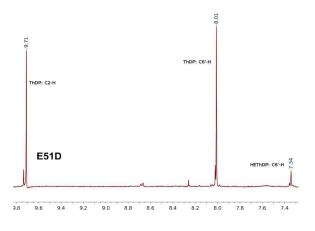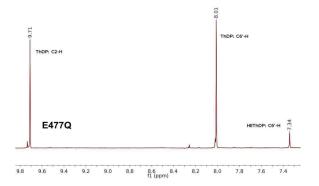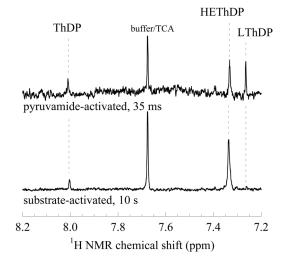
Figure 7.
Time course of 1′, 4′-iminoLThDP formation in YPDC and the E51D and E477Q active site variants with pyruvate under pre-steady state conditions. Enzyme (8 mg/mL) was rapidly mixed with 40 mM pyruvate in a Pi*-180 stopped-flow CD spectrometer and the CD signal was monitored at 313 nm. Data from 10 shots were averaged and the average was fitted to an exponential. The red trace for each spectrum is the regression fit line to double exponential. Top: YPDC (8 mg/mL) for 2 s at 10 °C. Middle: E477Q YPDC (8 mg/mL) for 50 s at 30 °C. Bottom: E51D YPDC (8 mg/mL) for 20 s at 30 °C.
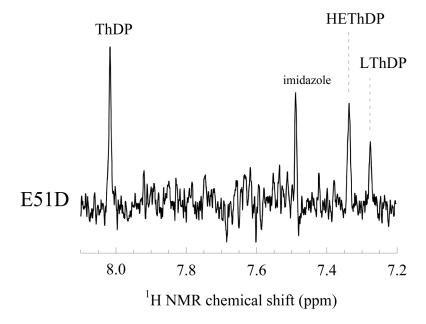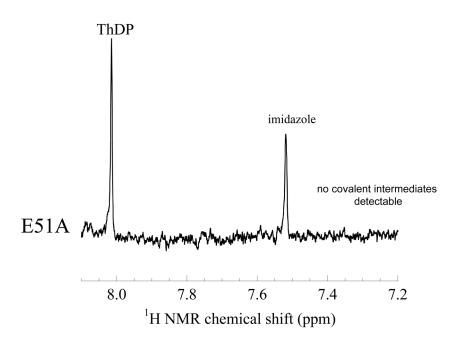
Figure 8.
^{1}H NMR detection of ThDP-bound intermediates under various conditions. Conditions of the steady-state CD titration experiment were replicated for: (Top) Reaction of E51D YPDC (25 mg/mL) with pyruvate (11 mM) at 5 °C was quenched with acid after 3 min. The supernatant containing the ThDP intermediates was analyzed by ^{1}H NMR using the characteristic C6′-H chemical shifts. [HEThDP]/[active sites] = 54.4% (determined from relative integrals of the corresponding signals after correction for excess ThDP from buffer). (Second from top) Reaction of E477Q YPDC (25 mg/mL) with pyruvate (11 mM) at 5 °C was quenched with acid after 3 min. [HEThDP]/[active sites] = 59%. (Bottom two): Distribution of covalent reaction intermediates in YPDC under steady state and transient

state conditions. YPDC was either preincubated with activator pyruvamide (100 mM) for 10 min before mixing with substrate, or, alternatively, directly reacted with pyruvate as detailed in ref. 16.

Figure 9.
Distribution of ThDP-bound intermediates during transient state of Glu51 variants. C6′-H fingerprint region in ^{1}H NMR spectra acquired with samples after acid quench of the reaction of (Top) E51D YPDC (5 mg/mL) at 0.035 s and (bottom) E51A (24 mg/mL) at 2 s with 100 mM pyruvate. All spectra were acquired at 25 °C and pH 0.75. Acquisition parameters are described under Experimental Procedures.

Scheme 1.
(A) Mechanism of catalytic cycle of yeast pyruvate decarboxylase. In bold font are the net forward rate constants for individual steps. The bold abbreviations APH⁺, AP and IP above each intermediate refer to the predominant ionization/tautomerization state of the 4′-aminopyrimidine in that particular intermediate. (B) Mechanism of formation of the 1′,4′-iminoPPThDP.

Table 1

Kinetic parameters for YPDC and its variants used in this study.

Variant	k_{cat} $(s^{-1})/^a$ subunit	n_H	$S_{0.5}$ (mM)
YPDC	60	1.88 ± 0.06	1.1 ± 0.2
E51D	0.049	1.39 ± 0.05	23.1 ± 1.3
E51Q	0.035	1.07 ± 0.08	14.9 ± 1.3
E51N	0.0024	1.34 ± 0.2	31.5 ± 12
E51A	0.0043	1.58 ± 0.2	0.72 ± 0.1
D28A	0.066	2.01 ± 0.16	1.66 ± 0.25^b
E477Q	0.086	1.49 ± 0.11	3.02 ± 0.22^b
E91D	11	1.86 ± 0.14	1.79 ± 0.22^c
C221E/C222A	18.2	1.05 ± 0.02	1.47 ± 0.04^d

[a] Per subunit, there are four subunits.

[b] From ref. 22.

[c] From ref. 29.

[d] From ref. 43. This is a double-mutant with a substitution at the neighboring Cys222 to eliminate potential complications. This substitution has no influence on the activity.

Table 2

Equilibrium binding parameters of PP to YPDC variants from CD.[a]

Variant	K_d^{app} (mM)	Hill coefficient, n_H	CD max (mdeg)
YPDC	9.1 ± 0.45 (MC)	2.13 ± 0.2 (MC)	− 6.65 ± 0.23 (MC)
	7.82 ± 0.55 (IP)	2.63 ± 0.45 (IP)	15.8 ± 0.79 (IP)
E91D	8.02 ± 0.92 (MC)	1.5 ± 0.2 (MC)	−2.85 ± 0.18 (MC)
	7.02 ± 1.34 (IP)	1.1 ± 0.16 (IP)	7.6 ± 0.63 (IP)
C221E	7.83 ± 3.48 (IP)	1.0 ± 0.22 (IP)	4.7 ± 0.77 (IP)
E51D	13.6 ± 0.35 (IP)	2.7 ± 0.2 (IP)	21.6 ± 0.54 (IP)
E477Q	Not detected		
D28A	Not detected		

[a]MC, Michaelis complex; IP, 1′,4′-iminopyrimidine tautomer of PPThDP.

Table 3

Observation of ThDP intermediates during various steps in catalytic cycle of YPDC.

	Thiazolium moiety	Aminopyrimidine moiety	Conditions where observed	Detection Method	Fig./Ref
1	Michaelis complex	APH⁺	YPDC+PP; E477Q/D28A + pyruvate steady state	CD, SF-CD	Figs. 3,4,5
2	LThDP	IP	YPDC+pyruvate transient state; E51D+pyruvate transient state	SF-CD, RCQ-NMR	Figs. 7,8,9
3	enamine	APH⁺	No direct detection with pyruvate		
4	HEThDP	IP	YPDC+pyruvate steady and transient states; E51D+pyruvate steady and transient states; E477Q +pyruvate steady state	CD, SF-CD, NMR	Figs. 2,6,7,8,9
5	ALThDP*	IP	D28A+pyruvate steady state	CD, NMR	Fig. 6; Ref. 16

*
C2-α-acetolactylThDP is an intermediate in acetolactate synthesis, which is a prominent side product of the D28A YPDC. It is not an intermediate in the YPDC catalytic cycle; however, it is relevant to the catalytic cycle of acetohydroxyacid synthase, a member of the ThDP superfamily.